

Synthesis of 5-[-2(3-Benzoyloxy-2-methylamino-propionylamino-3-methyl-pentanoylamino] 6-oxo-heptyl}-carbamic Acid 9H-fluoren-9-ylmethyl Ester (‘VAV-NH-(PEG)₂₃-NH-VAV’, the hydrogel) from NH₂(PEG)₂₃NH₂ and NCA VAV) and a Study of the Polymerisation Kinetics

Estella Judith Salamula^{1,*}, Misaël Silas Nadiye-Tabbiruka²

¹College of Natural Sciences, Department of Chemistry, Makerere University, Kampala, Uganda

²Department of Chemistry, University of Botswana, Botswana

Abstract Amine terminated Polyethyl glycol (NH₂(PEG)₂₃NH₂) and 4,8-diisopropyl-6-methyl-1,3,9-oxadiazecane-2,5,7,10-tetrone (NCA VAV) were used to synthesize the hydrogel 5-[-2(3-Benzoyloxy-2-methylamino-propionylamino-3-methyl-pentanoylamino] 6-oxo-heptyl}-carbamic acid 9H-fluoren-9-ylmethyl ester (‘VAV-NH-(PEG)₂₃-NH-VAV’). The hydrogel was characterized using proton and carbon NMR together with other spectroscopic techniques. The kinetics of the reaction were investigated in situ in an NMR tube in order to establish the mechanism of the polymerization of 4,8-diisopropyl-6-methyl-1,3,9-oxadiazecane-2,5,7,10-tetrone (NCA VAV with the di-functional diamide poly (ethylene) glycol, as an initiator. The reaction was found to proceed by 1st order mechanism with respect to the NCA VAV concentration.

Keywords Polyethylene glycol, Hydrogels, N-tert butoxycarbonanhydrides-(NCAs’), Polymerization kinetics

1. Introduction

Hydrogels can be physical, chemical in nature [1] or synthetic. A ‘chemical hydrogel is formed when polyelectrolytes and/or graft polymers of opposite charge precipitate depending on concentration, ionic strength and pH of the solution. Physical hydrogels are formed by 3D hydrophilic polymeric networks and are held together by their molecular entanglements and/ or secondary forces including H-bonding, or hydrophobic forces. These physical bonds, which hold them together, give rise to in-homogeneities as well as chain end defects or chain loops that represent transient network weaknesses in the physical gel.

Novel synthetically prepared proteins, like

5-[-2(3-Benzoyloxy-2-methylamino-propionylamino-3-methyl-pentanoylamino] 6-oxo-heptyl}-carbamic acid 9H-fluoren-9-ylmethyl ester (Poly VAV-PEGNH-VAV) amide are generally filed into libraries are classified in three groups namely: tryptic, semi-tryptic, and non-tryptic [2]. This classification allows peptides that belong to different tiers to have different “Bonferroni correction factors.” The scheme improves retrieval performance, significantly, compared to similar correction factors for all qualified peptides, according to their abilities.” [3-5] The wide range of synthetic techniques for peptides allows for the formation of 100-1000’s peptides via an automated sequencer. [6-8] This method has an added advantage over others in that it can be utilized to generate product libraries of high purity in solution and in solid state [9]. However, the main disadvantage is the tedious identifying technique, which necessitates coding and decoding [10].

Other techniques involve a combination of library techniques by mixing beads with peptides [11]. This technique yields reaction volumes in the range of 10⁷-10⁸

* Corresponding author:

matsciejs@gmail.com (Estella Judith Salamula)

Published online at <http://journal.sapub.org/ajb>

Copyright © 2017 Scientific & Academic Publishing. All Rights Reserved

peptides for biological and artificial blocks, which is considerably higher than wet synthesis. Condensation polymers include Polypeptides and polyesters, where water or methanol molecules are lost in the synthesis. However, other examples of condensation, such as acylation polycondensation of π -conjugated C-H bonds in aromatic monomers with dibromo-arylenes are attracting increasing attention as a simple synthetic method in which the preparation of organometallic reagents is not necessary [12].

These peptides are then filed into libraries that are split into small peptide mixtures with amino acids at certain spots [13]. The location of defined amino acids and mixed amino acids is known. Therefore all possible combinations are scanned/ screened and all randomized positions are de-convoluted by an interactive process based on library results. [14] Such proteins can then be grafted to Polyethylene glycol as blocks after forming the peptide or synthesized with the polyethylene glycol as an initiator, in much the same way I carried out the reaction.

A lot of work has gone into replicating proteins and hydrogels through synthesis using varying methods, forming libraries of these compounds. However, little is known about the kinetics of the reactions. Although the formation of polypeptides through *N-tert* carboxy anhydrides (NCAs) is widely known, and is currently used to prepare them, the kinetics and mechanism have received little attention. The only publication that delves into this kinetics study, appears to be that of Waley and Watson. They studied the polymerization of sarcosine *N*-carbonic anhydride and found the reaction to be complex. The reaction order with respect to (w.r.t) the monomer was initially more than 1 but eventually reached unity towards the end of the reaction, which differed with my NCA-VAV and amine terminated Poly glycol that I used for my experiment. However, when NCA was initiated with preformed polymer, the reaction order, w.r.t to the initiator concentration, was between 1-2 [15].

In this article, we report the synthesis and characterization of a chemical hydrogel, which can be used in repair and regeneration in heart tissue, from NCA-VAV and di-functional amine terminated polyethylene glycol (NH₂PEGNH₂) as initiator. We then investigate the kinetics of this polymerization reaction, utilizing magnetic resonance (NMR) at 600MHz.

2. Discussion

5-[2(3-Benzyloxy-2-methylamino-propionylamino-3-methyl-pentanoylamino) 6-oxo-heptyl]-carbamic acid 9H-fluoren-9-ylmethyl ester (Poly VAV-(PEG)₂₃-VAV amide)

¹H NMR (600 MHz, DMSO_{d6}): δ 0.89 [14H, t(*J*=7.4 Hz), β -(4CH₃O)] α -[2CH], 1.45 [6H,quartet(*J*=7.4 Hz), β -[2CH₃)], 1.72 [1H, q(*J*=6.6 Hz), α -(2CH), 2.55 [1H, t(*J*=7.4, 7.2 Hz), CH], 2.67 [1H, t(*J*=4.0 Hz), α -CH], 2.78 [1H, t(*J*=6.8 Hz), CH], 3.08 [1H, t(*J*=5.2 Hz), α -CH], 6.10 [1H, s, α -CH], 7.41 [1H, s, NH].

In the equation below, the di-functional amine (NH₂-(PEG)₂₄-NH₂) is used to polymerize the NCA-VAV, to form a hydrogel. Polymerization of NCAs' proceeds by cationic living mechanism and can be initiated with primary, secondary, tertiary amines and strong bases. [16, 17]. *Living polymerisation of NCA VAV to Poly VAV usually proceeds through carbamate and 'amine' or activated monomer mechanisms. Carbamate mechanism is initiated by a simple nucleophilic attack on the most acidic carbonyl, and water is released.* [18] (See Figure 1 for mechanism and then equation 1).

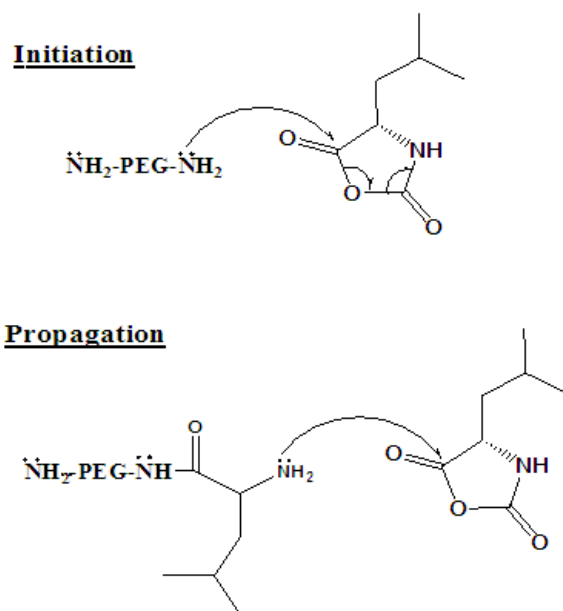
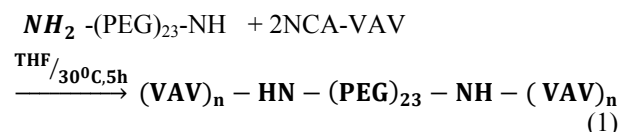


Figure 1. Illustration of the polymerisation mechanism of a single amino acid NCA



Equations 1: Polymerizing of NCA-VAV with (Amine terminated Polyethylene glycol)

Kinetics' analysis

Polymerization reaction kinetics can be investigated by utilizing a variety of techniques including GPC, electro-spray magnetic spectroscopy (ESMS), MALDI-TOF (in Figures 2-3) and proton nuclear magnetic resonance ¹H NMR. In this work, Proton NMR was utilized to follow the kinetics of this reaction in real time in situ. The ¹H NMR technique in particular has an added advantage in that the instrument can be modulated and/or manipulated to optimize the signal to noise ratio thus giving a clear picture of what is taking place in the reaction. This improved spectral resolution depends on homogeneity of the magnetic fields over the interrogated NMR sample volumes, hence the relatively low concentrations used in our experiment. However, commercial high-resolution NMR equipment is intended to have homogeneous magnetic fields over a large

area. So, any material introduced in the homogeneous area distorts the magnetic field unless the magnetic field can permeate through it easily.

The spectra, was recorded every thirty minutes, over a ten-hour period and all changes in intensity were tabulated and shown in figure 4. Three peaks with the most significant changes in intensity had broadened flat peaks, between for '4' and '10' at 8.36-8.4ppm and 'a & b' at 4.54-4.8ppm. Where the former peak depicts an amide functional group and the latter is the backbone of the polymer. However, functional groups between 0.5-3ppm are shown in the figure 5, as they are the most pictorial. There was a noticeable increase in intensity and broadening of the peaks, with an increase in M_w

of the polymer, as showed in Figure 4. The splitting of peaks '3' and '9' is due to (protons of the amide NH and methine CH group) and '6'(proton on the amide and methylene group CH_2); in the polymer.

DMSO can be found at 2.5ppm and the signal is usually a multiplet. In this case, the signal is a triplet, which indicates that there is something else under that peak. Furthermore, integration, showed more protons than were expected of DMSO alone. The triplet signal was also attributed splitting caused by the neighboring protons from the methyl (CH_3) and amide (NH)

MALDI spectra of VAV-NHPEGNH-VAV hydrogels

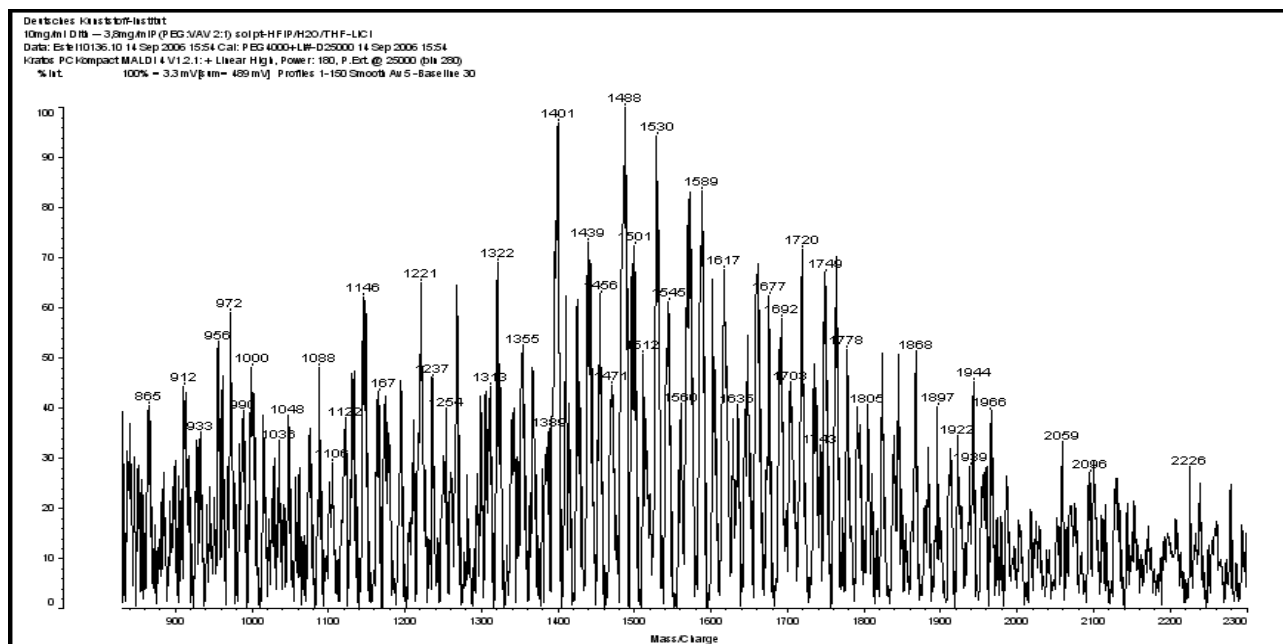


Figure 2. MALDI spectrum of 2PEG: 1VAV

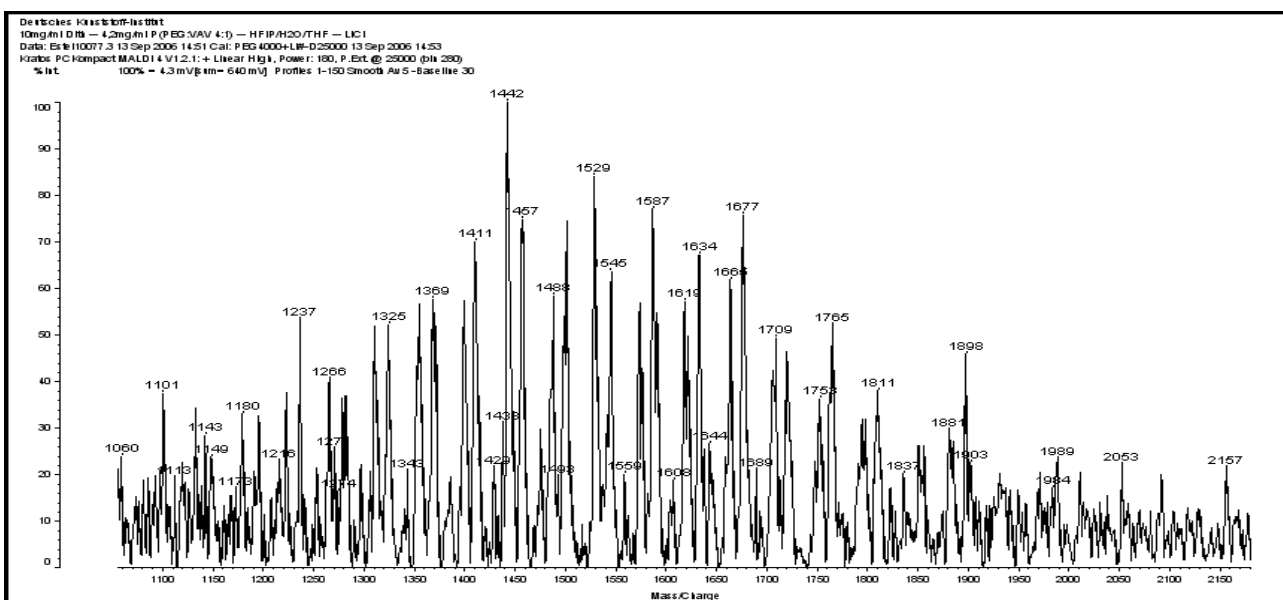


Figure 3. MALDI spectrum of (4PEG: 1VAV)

The parameters of the kinetics of the reactions were then obtained from the plots of intensity/concentration against time from the appropriate peaks.

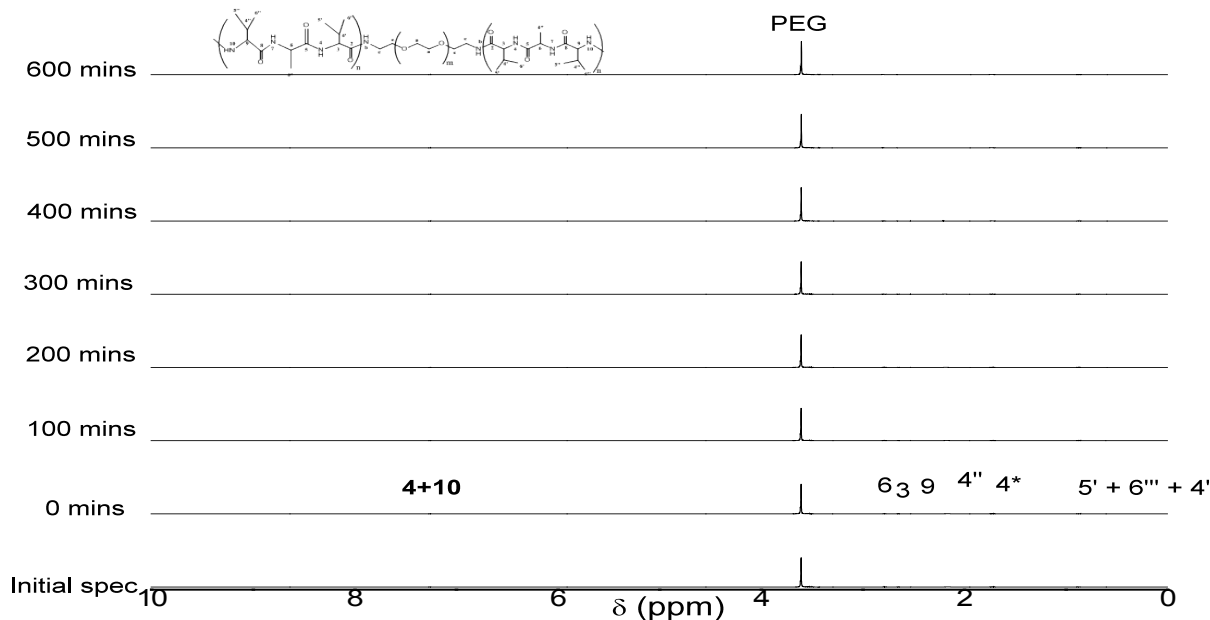


Figure 4. ¹H NMR spectra of reaction between NH₂-PEG-NH₂ with NCA-VAV against time (mins) (and enhanced spec from 3.0-0.5ppm below)

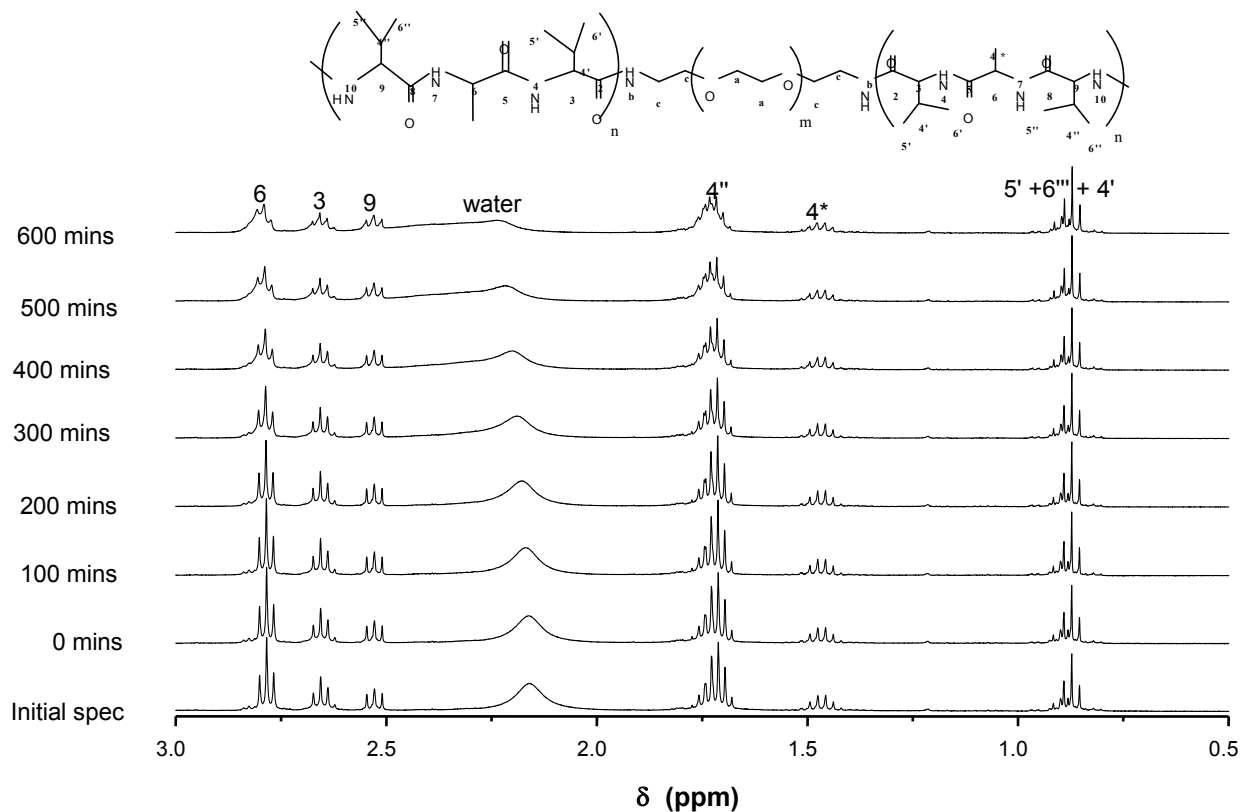


Figure 5. ¹H NMR spectra of reaction between NH₂-PEG-NH₂ with NCA-VAV over time (mins) and enhanced spec from 3.0-0.5ppm

Results were obtained as changes in intensity (and hence concentration, assuming Beer-Lambert's law holds at these low concentrations as it should) as a function of time, for the corresponding peaks such as those illustrated in Figure 5. Equation 2 was applied to both reactant group peak intensities and the results are presented in figure 8 for reactants and Figure 9 and Figure 10 for products.

$$\% = 100 - \left(\frac{I_x}{I_{start}} \right) \times 100 \quad (2)$$

I_x = reactant group intensity at any given time

I_{start} = reactant group intensity at start of the reaction

$$\text{Normalized reactant intensity}\% = (I_x/I_{start}) * 100 \quad (3)$$

Equation 3: Normalizing changes in reactant intensities during the reaction

Where I_{start} the initial intensity and I_x is the intensity, at any given time or concentration. This was taken for designated peaks over the time period. The value was then converted to concentration, since initial and final concentrations of the, 10-diisopropyl-3-methyl-1,4,7-triazecane-2,5,8,9-tetraone ('NCA-VAV') were already known. Since the I_x is smaller than I_{start} the result of equation 2 is a positive % hence we can take the log of the function.

Figure 8, shows the change in intensity/concentration ratio I_x/I_{start} of peaks 4", 5" and 6" in Figure 5 during the grafting of NCA-VAV onto the H_2N (PEG)₂₃ NH_2 , captured as a function of time, over 10 hours of polymerization. The reaction was initiated as the temperature of the mixture was brought to room temperature (25°C) from 0°C. Propagation and termination (tailing off) occurred when 6, 10-diisopropyl-3-methyl-1,4,7-triazecane-2,5,8,9-tetraone (NCA-VAV) monomer was exhausted. The overall reaction is 'bimolecular' probably complex with several steps in the mechanism. Hence, the rates of reaction of the various steps may vary. However, the method was chosen in order to obtain the reaction order, and can be obtained by plotting $\log(1 - (I_x/I_{start}) * 100)$ against concentration, where a straight line would indicate a first order process at the rate-determining step. The rate of depletion of NCA-VAV as a function of time is obtained by measuring the slope of the tangents of the curve in figure 8 as a function of time or by differentiating the equation of the fitted polynomial with respect to time and substituting in the specific times in the obtained equation, using linear regression equation 4. [19]

$$y_i = \beta_1 x_{i1} + \dots + \beta_p x_{ip} + \epsilon_i = \mathbf{x}_i^T \boldsymbol{\beta} + \epsilon_i, \quad i = 1, \dots, n, \quad (4)$$

Where T denotes the transpose, so that $\mathbf{x}_i^T \boldsymbol{\beta}$ is the inner product between vectors \mathbf{x}_i and $\boldsymbol{\beta}$.

This is a common statistical model fit that takes all the data points into account. The accuracy of the data was correlated using a co-efficient 'R²' and gave a positive result of 0.81, where 1 is complete unity.

The digital photo of the hydrogel is shown in Figure 7, some several years after it was synthesized. So it is quite hard in appearance and texture.



Figure 7. Poly (VAV-PEG-VAV) amide, some ten years after it was synthesized

The results were tabulated as, 'changes in intensity (/concentration) over time.' This is shown in figure 8.

Figures 9 and 10 show the increase in intensity and the concentration respectively, of methyl and methylene side groups in polymer with time. The concentrations can be represented by the polynomials:

$$Y = 7E-19x^2 + 2E-18x + 3E-12 \quad (5)$$

For the CH₃ and

$$Y = 8E-20x^2 + 4E-17x + 2E-13 \quad (6)$$

For the increase in concentration of the α -CH functional group in the main chain (see figure 11).

The graph in Figure 11 represents the percentage increase in the main chain, as a function of time. In this case y is an increase in percentage intensity/concentration and x is the time.

The order with respect to a reactant at the rate-determining step was determined by analyzing data of the effect of reactant concentration on reaction rate.

If Rate = k*(concentration of a reactant)ⁿ then

Log of rate = log k + n log (reactant concentration (or intensity function)).

Consequently a plot of log of rate against log of concentration should provide a straight line with a slope = n the order with respect to the reactant. In the polymerization reaction, in this work a straight line was indeed obtained and the order was found to be one (see Figure 12 and equation 13).

$$Y = 1.0213x + 3.9406 \quad (7)$$

Equation 7: Rate of reaction

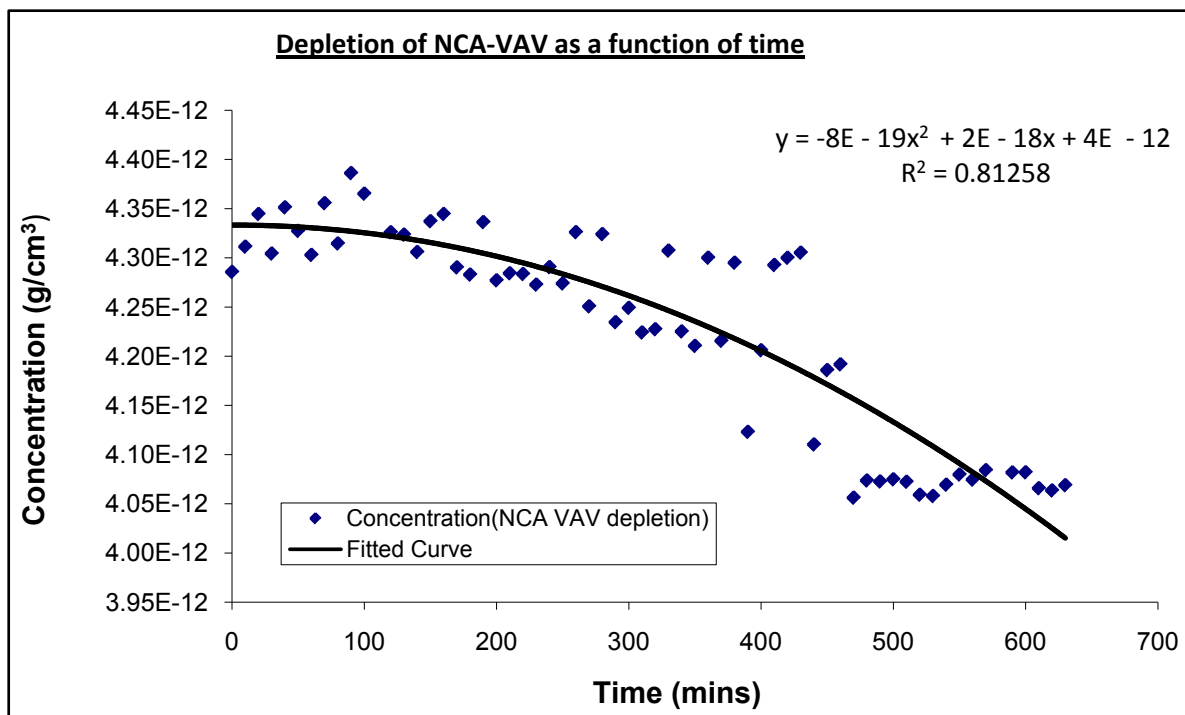


Figure 8. Depletion of NCA-VAV as a function of time with respect to concentration

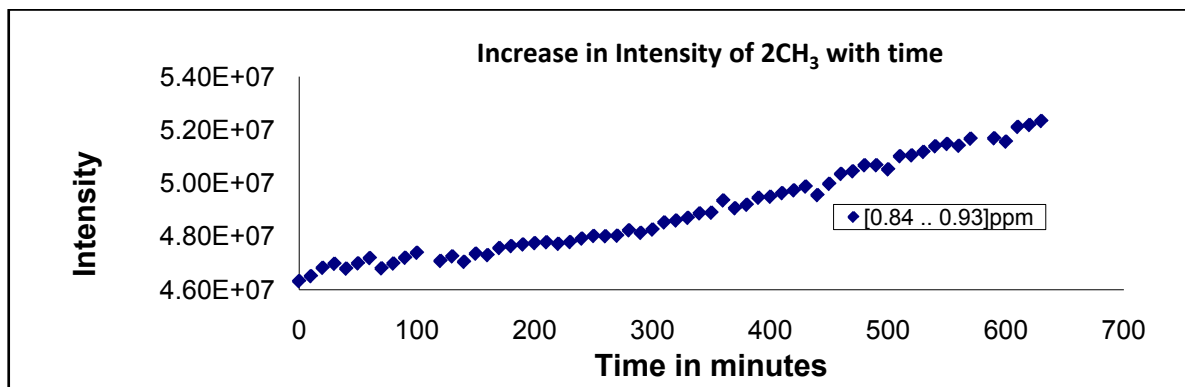


Figure 9. Shows the variation of product group intensity during grafting polymerization of NCA (VAV). With NH-(VAV)₂₃-NH₂ as a function of time with time

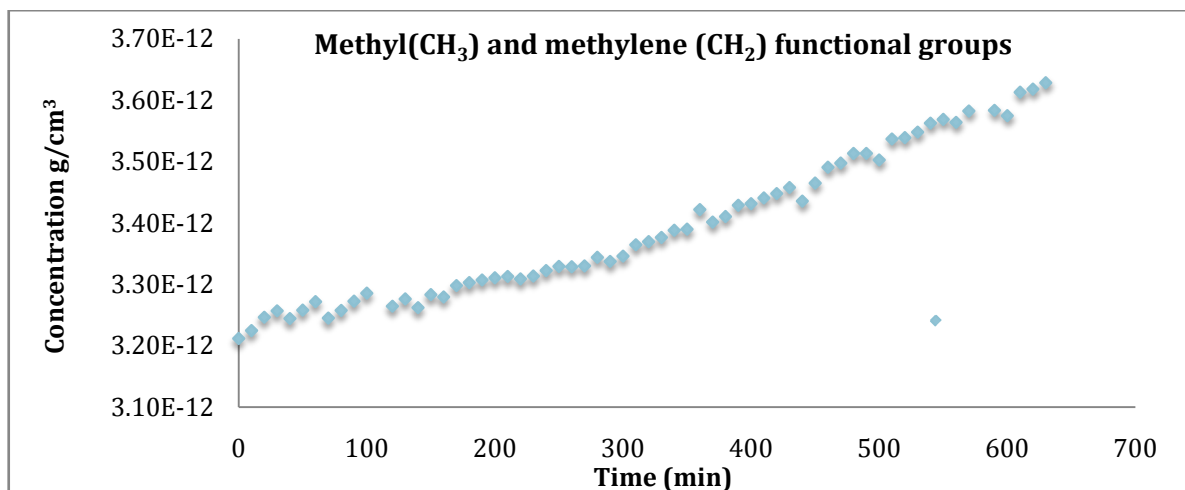


Figure 10. Illustration of change in product group concentration during grafting polymerization of NCA (VAV). With NH₂-(VAV)₂₃-NH as a function of time

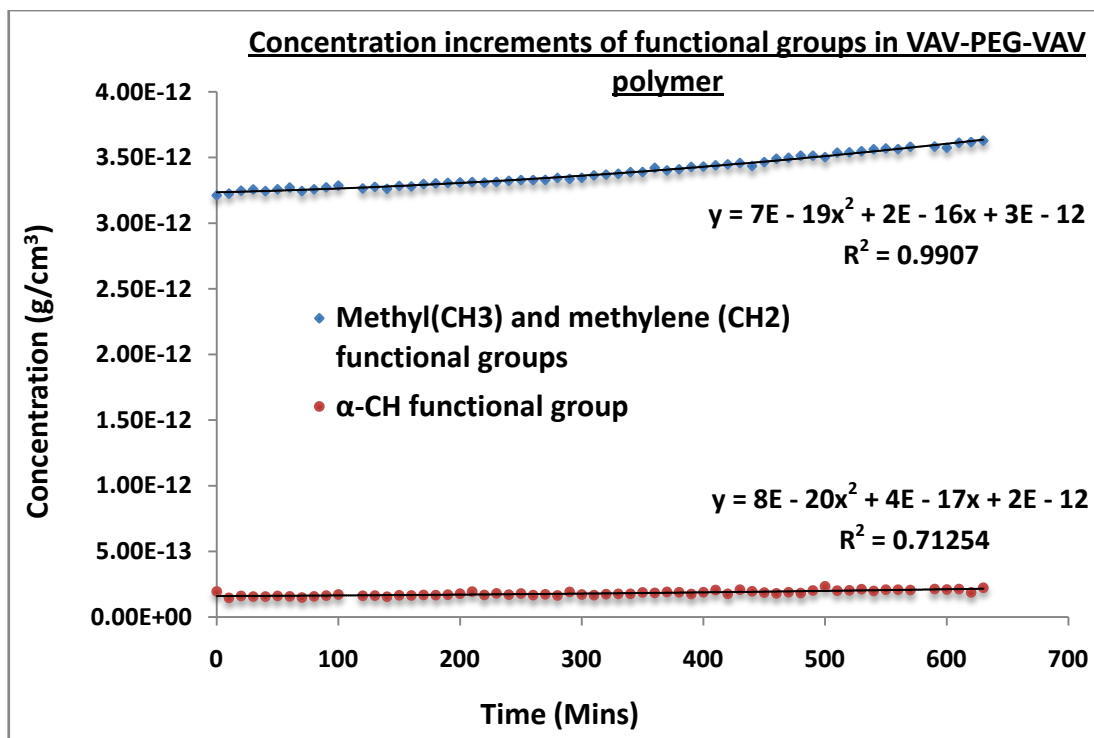


Figure 11. Study of the rate of reaction of Poly (VAV) amide onto amine terminated PEG as a function of time

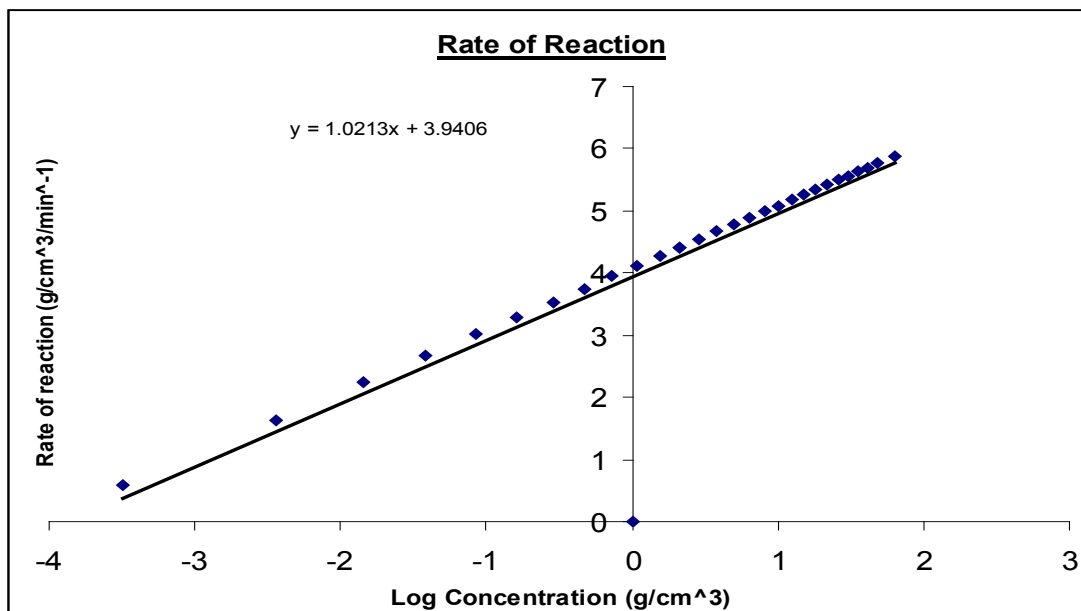


Figure 12. Rate of reaction of the NCA-VAV depletion as a function of Log concentration

3. Experimental

3.1. Equipment

Melting point apparatus (DMA 8000): for melting point determination; TLC paper was used to obtain $-R_f$ values.

Nicolet Nexus Fourier-Transform infrared (FTIR): 'for obtaining fingerprint' spectrums of molecules.

Oxford-NMR (300/400/600MHz Agilent) was used for Carbon and proton Nuclear Magnetic resonance spectra and

CapLC-QTOF Ultima ESMS-Electrospray mass spectrometer was used to obtain molecular masses.

3.2. Materials

Alanine, valine, thionyl chloride, oxalyl chloride, methanol, 4-*tert*-butoxycarbonyl, lithium hydroxide, potassium sulphate, magnesium sulphate, sodium bicarbonate and sodium hydroxide were obtained from Sigma Aldrich; hydroxybenzotriazole (HoBt), silica gel,

O-(Benzotiazole-1-yl)-N'N'N'N'-tetramethyluronium tetrafluoroborate (TBTU) were obtained from Advanced ChemTech, South Africa and were used without further purification. THF, DMF, acetonitrile and ethanoic acid, diisopropyl ethylamine were purified by re-distillation before use. Water was obtained from an onsite distilling and de-ionizing system.

3.3. Procedure

Polymerizing of NCA VAV on NH₂-(COCO)₂₃-NH₂

The experiment was conducted in an NMR tube, in which 0.075 mmol of freeze dried NH₂-(PEG)₂₃-NH₂ and 0.3 mmol of NCA-VAV were added and allowed to polymerize over a period of 10 hours, in deuterated chloroform. The 'polypeptide grafting reaction' was followed by capturing spectral data every 30 min. All changes in intensity were tabulated. Three peaks with significant changes in intensity were studied, tabulated and their intensities plotted as a function of time/concentration. Details of the NMR characterization are listed in the results section.

ACKNOWLEDGMENTS

The authors wish to acknowledge the contributions from the Department of Chemistry and Polymer science of the University of Stellenbosch in South Africa for the lab space, chemicals and equipment used. The contribution by the laboratory staff is also greatly appreciated.

Abbreviations

6,10-diisopropyl-3-methyl-1,4,7-triazecane-2,5,8,9-tetraone/ NCA VAV, Melting point/M.P, Thin layer Chromatography/TLC; Ultra-violet/UV, Infra-red/IR, Nucleic magnetic resonance/NMR; Electrospray mass spec/ESMS.

REFERENCES

- [1] Wong Po F., C. T. S., Leea, J. S., Mulyasasmitab, W., Parisi-Amonb, A., 2009, PNAS, 106, 52 22067.
- [2] Wind, M., Gosenca, D., Kübler, D., 2013, Anal. Biochem., Stable isotope phosphor-profiling of fibrinogen and fetuin subunits by element mass spectrometry coupled to capillary liquid chromatography, 317, 1, 26-33.
- [3] Alves, G. and Yu, Y. K., 2013, J. Proteome Res., 12, 6, 2571.
- [4] Hurevich, M., Barda, Y.; Gilon, C., 2007, Heterocycles, 73, 617.
- [5] Reporters at Hispanic Business., 2014, http://www.hispanicbusiness.com/2014/7/16/recent_findings_in_peptides_and_proteins.htm.
- [6] Blanchard, R., 2013, <http://www.extremepeptides.com/blog/brix/>.
- [7] Bacchi, M., Fould, B., Jullian, M., Kreiter, A., 2017, Anal. Chem., Screening ubiquitin specific protease activities using chemically synthesized ubiquitin and ubiquitinatedpeptides, 517, 57-70.
- [8] Hochscherf, J., Lindenblatt, D., Steinkrüger, M., Yoo, E. M., and Pietsch, M., Anal. Chem., 2015, Development of high-throughput screening-compatible assay to identify inhibitors of CK2 α /CK2 β Interaction, 468, 4-15.
- [9] Lipinski, C. A., 2004, Technologies, 1, 4,337.
- [10] Liu, R., Marik, J., Lam, K. S., 2002, J Am Chem Soc., 124,26, 7678.
- [11] Brown, J. M., Hoffmann, W. D., Alvey, C. M., Verbeck, G. F., 2010, Anal. Biochem., 398, 1, 7.
- [12] Seong, J., 2013, 'Microwave-Assisted Polycondensation via Direct Arylation of 3,4-Ethylene dioxithiophene with 9,9-Dioctyl-2,7-dibromofluorene,' *Chem. Eng.*, 2013, 1 (8), 878-882.
- [13] Lam, K. S., Lebl, M., and Krchn'ák, V., 1997, Chem. Rev., 97, 411.
- [14] Low, C. M. R., 1995, Ultrason. Sonochem., 2, 2, S153.
- [15] Waley, S. G and Watson, J., Recueil des Travaux Chimiques des Pays-Bas., 1950, 69, 1, 27.
- [16] Matyjaszewski K. (2007), "Erratum to: "Controlled/living radical polymerization: Features, developments and perspectives," Prog. Polym. Sci., 33, 93.
- [17] Deming T. and Curtain S. A., (2000), 'Chain Initiation Efficiency in Cobalt- and Nickel-Mediated Polypeptide Synthesis', J. Am. Chem.Soc., 122, 5710.
- [18] Salamula, E. J and Nadiye-Tabbiruka, M. S.; (2015) Optimizing of N'-tert-butoxycarbon anhydrides polymerization of NCAs' AG, SIK and VAV, Int. J. Appl. Chem. 2015, 11, 4, 409-426.
- [19] Rencher, A. C., Christensen, W. F., 2012, Introduction", Methods of Multivariate Analysis, Wiley Series in Probability and Statistics, "Chapter 10, Multivariate regression – Section.